THE ANALYSIS OF STABLE CRACK GROWTH IN TYPE 304 STAINLESS STEEL

S. G. Sampath, I. S. Abou-Sayed, D. Broek, C. Marschall,
A. Zahoor and M. F. Kanninen

BATTELLE
Columbus Laboratories
Columbus, Ohio, USA

ABSTRACT

The objective of the research described in the paper is to develop a plastic fracture mechanics approach to assess the load carrying capacity of austenitic steel pipes used in nuclear plants. Experimental crack growth data have been acquired in conjunction with elastic-plastic finite element analysis results to develop crack growth resistance curves for Type 304 stainless steel, based on the J-integral and the crack tip opening angle. Results indicate that a resistance curve obtained under monotonic loading will be applicable to cyclic or seismic loading conditions also.

KEYWORDS

Plastic Fracture Mechanics, stainless steel, crack growth resistance curves, experimental data, seismic loading, finite element analysis.

INTRODUCTION

Cracks that have occurred in the heat-affected zones of girth welds in some Type 304 stainless steel pipes are a concern in boiling water reactor (BWR) nuclear plants. These cracks initiate at the inner surface of the pipe wall and grow radially and circumferentially due to the combined action of stress corrosion and fatigue. While no serious accidents have yet been caused because of such cracks, the possibility exists that a higher than operating load, perhaps generated by a seismic event, could result in pipe fracture.

The basic reason that pipes made of tough materials like Type 304 stainless steel exhibit considerable strength even when large cracks exist is due to the large amount of plastic deformation that precedes the initiation of crack growth. In addition, because stable crack growth usually follows initiation, the maximum load carrying capacity of the pipe can be greater than the load required to initiate growth. Conventional fracture mechanics techniques do not take crack blunting and stable crack growth into account, thus underestimating the maximum load that the pipe can sustain. To obtain more precise determinations, a plastic fracture mechanics approach must be employed.

This paper describes the basis of a plastic fracture mechanics approach to obtain quantitative assessments of crack initiation and growth in ductile materials. Specifically, experimental crack growth data have been acquired in conjunction with elastic-plastic finite element analyses to develop an appropriate resistance curve for Type 304 stainless steel. This will permit detailed crack propagation computations to be made for flawed reactor piping.

Previous research (Kanninen and colleagues, 1978) has suggested that a net section collapse criterion can be used to easily obtain reasonably accurate estimates of the failure load in circumferentially flawed pipes. The behavior of the center-cracked-tension specimens (CCT) described in this report offers further support for the collapse criterion, albeit geometry dependent; i.e., whether the loading is monotonic or cyclic. But a fundamental approach such as pursued under the current research program can better define the realm of applicability of this criterion for pipe instability predictions.

The content of this paper is a part of a wider analytical-experimental program that includes assessments of growth of through-wall and part-through wall circumferential flaws in large diameter pipes made of Type 304 stainless steel under static and dynamic loading conditions. The research reported here is still in an early stage. Nevertheless, some important results have been obtained. The most significant result pertains to the use of a J-resistance curve for the determination of crack growth and fracture under seismic conditions. Specifically, the three-point bend test results reveal that Type 304 stainless steel exhibits nearly the same resistance at a high (impact) loading rate as in quasi-static loading. Further, the results of cyclic, interrupted, and seismic simulation tests on center-cracked panels also indicate that a resistance curve obtained under monotonic loading will adequately characterize this material. However, it should also be noted that specimens tested at operating temperature exhibit a lower resistance than those at room temperature. Hence, this effect cannot be neglected for a conservative assessment.

THREE-POINT BEND SPECIMEN TESTING

Sharp-notch 3-point bend tests were conducted to assess the influence of specimen thickness, test temperature, and loading rate on the initiation and stable growth of cracks in Type 304 stainless steel. In addition, a limited amount of work was performed to verify that sharp machined notches adequately simulate actual stress corrosion cracks.

Specimens with thickness (B) of 8 mm and 25 mm, respectively, were examined as approximations to the wall thicknesses of 10-cm and 66-cm diameter Schedule 80 pipes. Tests at both room temperature and at 290C were conducted. To evaluate loading rate effects, two load-point displacement rates, viz., 9 x 10^{-6} m/sec and 1.8 m/sec, were employed.

The notched 3-point bend specimens were patterned after the standard dynamic tear specimen (ASTM, 1979a) with the ratio of span to width being close to the value of 4 recommended for J_{Ic} tests (ASTM, 1979b). The bend tests at low rates were conducted on an Instron testing machine while the high rate tests were carried out using a drop weight impact tester. During low rate tests the average crack extension was measured by means of the unloading compliance method. In addition, close up photographs were obtained to permit measurement of surface crack lengths and the crack opening displacements. After the crack had extended about 10 mm, the specimen was unloaded, heat tinted to define the crack profile, and broken open.

The multiple-specimen method was employed in the high loading rate tests. The amount of crack extension in individual specimens was controlled by stopping the falling weight after a predetermined amount of deflection. The crack opening displacement (COD) and the midspan displacements were measured from photographs and the average crack extension was measured after heat tinting and fracturing the specimen completely.

Figure 1 illustrates the relation among load, load-point displacement, and crack extension in a typical low rate test. Figure 2 shows the same type of relationship under high rate loading. From experimentally measured values of load, midspan deflection, and average crack length, the method given in (Garwood, Robinson and Turner, 1975) was used to construct the J-resistance curves shown in Figs. 3 and 4.

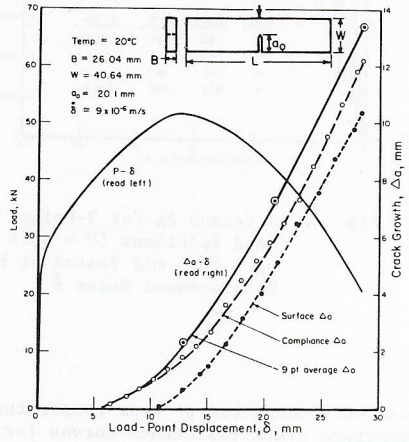

Fig. 1. Results of Low Rate Test on Sharp-Notched 3-Point Bend Specimens Illustrating Δa Values Obtained by Several Methods

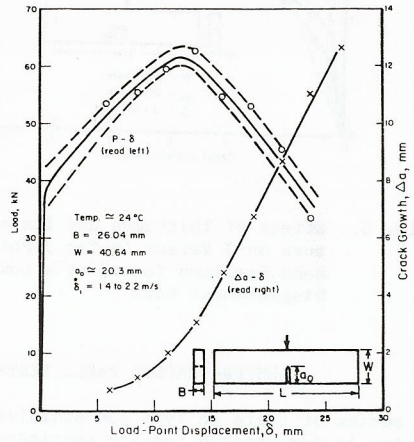

Fig. 2. Results of Interrupted Impact Tests on Sharp-Notched 3-Point Bend Specimens

Figures 3 and 4 show that the J-resistance curves for the specimens tested under impact loading conditions were higher than those generated under slow rate loading conditions. Recent work (Paris, et al, 1979) has shown that both J and dJ/da are essential in determining if crack growth instability will take place. For the same J, a higher dJ/da will have a higher resistance to cracking. It can be seen from Figures 3 and 4 that the specimens tested under impact loading conditions show higher dJ/da values than the specimens tested under slow rate loading. Based on this criterion, the use of the J-resistance curve generated under slow loading rates to predict crack growth instability will underestimate the load carrying capacity for impact loading situations.

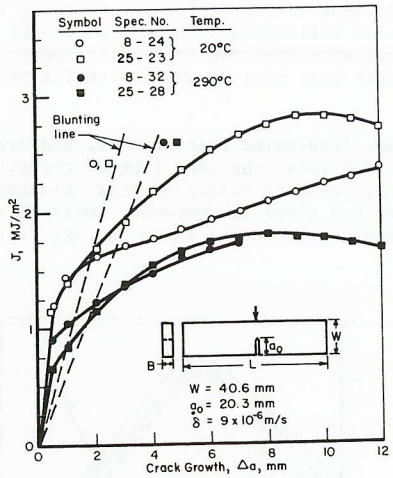

Fig. 3. Effect of Thickness and Temperature on J Versus Δa for 3-Point Bend Specimen Tested at a Low Displacement Rate

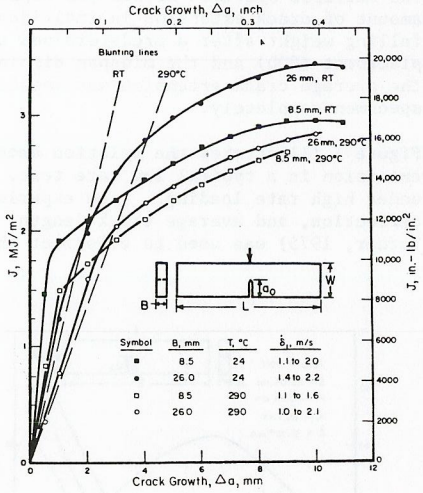

Fig. 4. J Versus Δa for 3-Point Bend Specimens (W = 40.6 mm, a_o = 20.3 mm) Tested at High Displacement Rates $\dot{\delta}$

CENTER-CRACKED PANEL TESTS

A series of tests on Type 304 stainless steel were conducted at room temperature using center-cracked tension specimens to generate crack resistance curves for seismic loadings. A secondary purpose of the tests was to provide guidelines for establishing simplified load histories that could be used in analytical models. To achieve these objectives, tests were performed using increasingly complex load histories. In a number of tests the load was released and incremented several times during crack growth. Some tests were conducted with batches of 20 to 50 constant-amplitude-load cycles applied at various stages of crack growth. Finally, tests were performed in which a seismic load sequence, based on an actual seismic record, were repeatedly applied.

Each of the specimens were 304 mm wide, 1215 mm long, and 8.3 mm thick. Accounting for the grip arrangement, the free length was 608 mm. The crack opening displacement and the displacement component near the grips were recorded. Additionally, displacements throughout the plate were indirectly monitored through film records of positions of grid lines scribed on the panels. Strain gages at selected locations were also a part of the instrumentation. A summary of the test conditions and results is contained in Table 1. The sequence corresponding to the seismic loading case is shown in Fig. 5.

TABLE 1 Crack Size and Applied Stress at Crack Initiation and Maximum Load - Flat Plate Experiments

Spec. No.	Load or Strain Control	Crack Length at Initiation		Crack Length at Max. Load		Applied Stress at Initiation		Applied Stress at Max. Load		Remarks
		mm	in.	mm	in.	MPa	ksi	MPa	ksi	
1	Strain	41.9	1.65	54	2.14	388	56.0	423	61.16	normal
2	Strain	76.2	3.00	91	3.62	302	43.7	322	46.58	normal
4	Strain	76.2	3.00			356	51.4	377	54.5	strain rate
6	Strain	76.2	3.00	89	3.49	322	46.6	345	50.0	interrupted
8	Load	76.2	3.00	100	3.94	338	48.8	368	53.2	cyclic
9	Strain	76.2	3.00	90	3.55	328	47.5	346	50.0	cyclic
10	Load	76.2	3.00	89	3.49	328	47.5	348	50.3	cyclic
14	Load	76.2	3.00	90	3.55	332	48.0	354	51.1	sensitized
15	Load	76.2	3.00	93	3.66	347	50.2	365	52.7	seismic
16	Load	76.2	3.00	86	3.39	339	48.9	368	53.2	seismic
18	Strain	76.2	3.00	90	3.60	338	48.9	355	51.2	seismic
19	Load	76.2	3.00	89	3.50	328	47.4	340	49.2	seismic
3	Load	133.3	5.25	151	5.94	258	37.2	274	39.5	normal
5	Strain	133.3	5.25			278	40.1	290	42.0	strain rate
7	Strain	133.3	5.25	145	5.69	259	37.4	273	39.5	interrupted
11	Strain	133.3	5.25	148	5.81	260	37.5	280	40.4	cyclic
12	Load	133.3	5.25	146	5.75	254	36.7	275	39.8	cyclic
13	Strain	133.3	5.25	146	5.74	247	35.8	266	38.3	sensitized
17	Load	133.3	5.25	146	5.75	253	36.7	276	39.8	seismic
20	Load	133.3	5.25	145	5.64	238	34.4	261	37.8	seismic

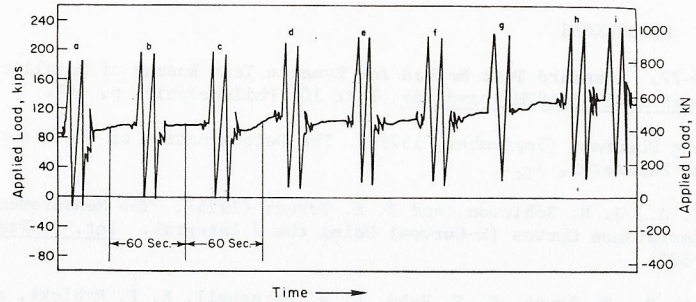

Fig. 5. Seismic Events of Increasing Severity Applied to Flat Plate (Specimen No. 16 in Table 1)

It was observed that stable crack propagation took place on a plane perpendicular to the plate surface, whereas unstable fracture was of the slanted variety. In general, instabilities did not occur under stroke control conditions, while unstable fractures of the slant type were associated with the load control tests. Extensive thinning of the plate occurred in the vicinity of the crack tip in each case. Figures 6 and 7 show typical load-COD records of cyclic load tests performed under stroke-controlled and load-controlled conditions. The essential result emerging from the test series is that the crack growth behavior under interrupted or seismic loading very nearly corresponds to the curves obtained under monotonic conditions.

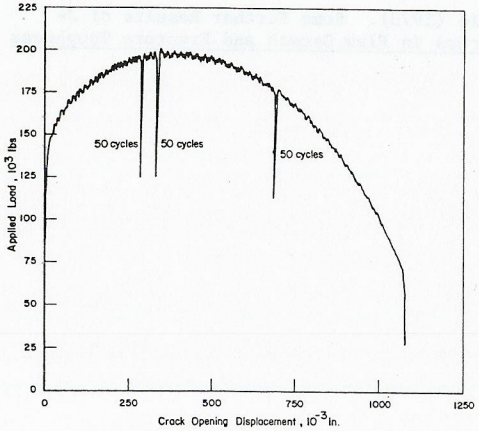

Fig. 6. Applied Load Versus Crack Opening Displacement Curve for a Flat Plate Specimen with a 3.00 Inches Central Notch Under Interrupted Fatigue Loads - Stroke Control

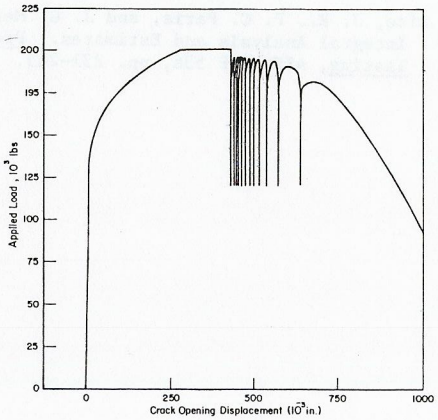

Fig. 7. Applied Load Versus Crack Opening Displacement Curve for a Flat Plate Specimen with a 3.00 Inch Central Notch Under Interrupted Fatigue Loads - Load Control

FINITE ELEMENT ANALYSES OF STABLE CRACK GROWTH

A general purpose, finite element computer program, BCLFEM, was used to model some of the tests described earlier. Because of the very large strains accompanying deformations in Type 304 stainless steel, a large deformation-finite strain formulation was incorporated in BCLFEM. The equations underlying the finite strain formulation may be found in (McMeeking and Rice, 1975). The rate problem defining the deformation tensor is based on an updated Lagrangian scheme and the Jaumann rate of the Kirchhoff stress. A subroutine to calculate the J-integral for user defined paths, consistent with the activation of the finite strain formulation is a part of BCLFEM. The material stress-strain curve was represented as multilinear (six segments), using experimentally derived Cauchy stress-logarithmic strain curve.

"Generation" phase analyses that have been carried out involved the use of experimentally derived load versus crack growth curve to simulate crack extension. Specifically, incrementation of the crack length was effected through dissipation of the force at the crack tip node to zero. Validation of the analytical model was made through comparisons of the computed compliance of the specimen and of the computed strain/displacement values obtained against experimental data.

To date, only the 8 mm thick plates have been modelled using the plane stress formulation. Figure 8 corresponds to the case of a center-cracked panel under monotonic loading. The initial flaw size for this case was 7.62 cm. Figure 8 shows the comparison between experimental data and the numerically computed load P at the symmetry point where the remote displacements were applied.

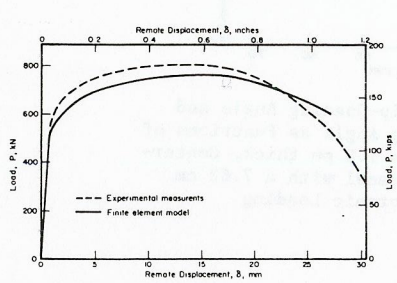

Fig. 8. Compliance of a 7.9 mm thick, Center-Cracked Tension Panel with a 7.62 cm Notch, Under Monotonic Loading

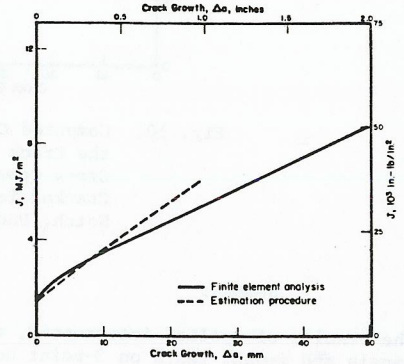

Fig. 9. Computed J-Resistance Curve for a 7.9 mm Thick, Center-Cracked Tension Panel with a 7.62 cm Notch, Under Monotonic Loading

The J-integral was calculated following five separate contours. Up to the maximum load, the J-Δa (Δa = crack extension) curves for the five contours are almost identical. But, soon after, they begin to show path dependence. Comparison between the J-resistance curve using the estimation scheme given in (Rice, Paris and Merkle, 1973) and the finite element computations (Fig. 9) showed good agreement until the maximum load point. This is in conformity with recently reported

observations. The value of J at maximum load was calculated as 3.28 MJ/m^2 which corresponds to a remote displacement, δ, equal to 14.8 mm.

Figure 10 shows the COA and CTOA as a function of the load, also for a center-cracked panel. It can be seen that the COA continously decreases with growth, whereas the CTOA, after an initial transient, attains a plateau value of about 0.27 radians. The crack tip opening displacement was calculated to be 2.84 mm, a value that agrees well with the experimental result. Because of the limitation to small amounts of crack growth that exists for the J-resistance curve approach, the combined J/CTOA approach suggested in (Kanninen and colleagues, 1980) appears to be a possible way of coping with extended amounts of stable growth that might precede fracture instability.

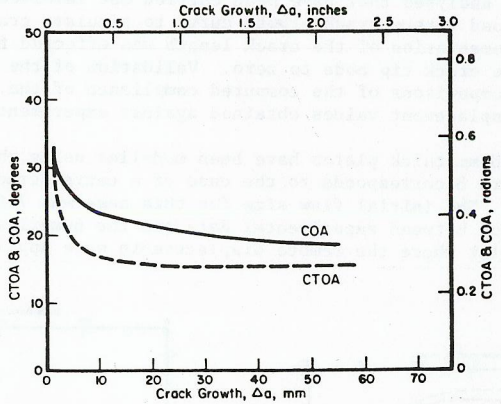

Fig. 10. Computed Crack-Tip-Opening Angle and the Crack Opening Angle as Functions of Crack Growth in a 7.9 mm thick, Center-Cracked Tension Panel with a 7.62 cm Notch, Under Monotonic Loading

SUMMARY

The results of cyclic, interrupted, and seismic simulation tests on center-cracked panels and impact tests on 3-point bend specimen indicate that a quasi-static resistance curve obtained under monotonic loading will adequately characterize Type 304 stainless steel. The J-resistance curve can apparently be used for determining initiation of crack growth and some small amount of stable crack growth.

ACKNOWLEDGMENT

These results were obtained in a research program (T118-2) supported by the Electric Power Research Institute, Palo Alto, California. The authors would like to thank Drs. Robin Jones and Douglas Norris, Jr. for their help and encouragement.

REFERENCES

ASTM E 604-77. Standard Test Method for Dynamic Tear Energy of Metallic Materials. 1979 Annual Book of ASTM Standards, Part 10, Philadelphia, p. 645.

ASTM Working Document (September, 1979). The Determination of the Elastic-Plastic Toughness Parameter, J_{Ic}.

Garwood, S. J., J. N. Robinson, and C. E. Turner (1975). The Measurement of Crack Growth Resistance Curves (R-Curves) Using the J Integral. Int. J. Fracture, 11, pp. 528-532.

Kanninen, M. F., D. Broek, G. T. Hahn, C. W. Marschall, E. F. Rybicki, and G. M. Wilkowski (1978). Towards an Elastic-Plastic Fracture Mechanics Capability for Reactor Piping. Nuclear Engineering and Design, 48, pp. 117-134.

Kanninen, M. F., G. T. Hahn, D. Broek, R. B. Stonesifer, C. W. Marschall, I. S. Abou-Sayed, and A. Zahoor (1980). Methodology for Plastic Fracture - Phase II. Battelle's Columbus Laboratories Final Report to EPRI, Columbus, Ohio.

McMeeking, R. M. and J. R. Rice (1975). Finite Element Formulation for Problems of Large Elastic-Plastic Deformations. Int. J. Solids Struct., 11, pp. 601-616.

Paris, P. C., H. Tada, A. Zahoor, and H. Ernst (1979). The Theory of Instability of the Tearing Mode of Elastic-Plastic Crack Growth. In J. D. Landes, J. A. Begley, and G. A. Clarke, (Eds.), Elastic-Plastic Fracture, ASTM STP 668, American Society for Testing and Materials, pp 5-36.

Rice, J. R., P. C. Paris, and J. G. Merkle (1973). Some Further Results of J-Integral Analysis and Estimates. Progress in Flaw Growth and Fracture Toughness Testing, ASTM STP 536, pp. 231-245.